

NeuroPilot: A Realtime Brain-Computer Interface system to enhance concentration of students in online learning

Asif Islam, Farhan Ishtiaque, Md. Muhyminul Haque, Kaled Masukur Rahman, Ravi Vaidyanathan, and Khondaker Abdullah-Al-Mamun

Abstract—Prevalence of online learning poses a vital challenge in real-time monitoring of students’ concentration. Traditional methods such as questionnaire assessments require manual interventions and webcam-based monitoring fails to provide accurate insights into learners’ mental focus as they are deceived by mere screen fixation without cognitive engagement. Existing BCI-based approaches lack real-time validation and evaluation procedures. To address these limitations, a Brain-Computer Interface (BCI) system is developed using a non-invasive Electroencephalogram (EEG) headband, FocusCalm, to record brainwave activity under attentive and non-attentive states. 20 minutes of data were collected from each of 20 participants watching a pre-recorded educational video. The data validation employed a novel intra-video questionnaire assessment. Subsequently, collected signals were segmented (sliding window), filtered (butterworth band-pass), and cleaned (removal of high-amplitude and EOG artifacts such as eye blinks). Time, frequency, wavelet and statistical features have been extracted, followed by recursive feature elimination (RFE) with Support vector machines (SVMs) to classify attention and non-attention states. The leave-one-subject-out (LOSO) cross-validation accuracy has been tested to be 88.77%. The system provides feedback alerts upon non-attention state detection and keeps focus profile logs. A pilot study was conducted to evaluate the effectiveness of real-time feedback. Five participants completed a 10-minute session consisting of a 5-minute baseline phase without feedback followed by a 5-minute feedback phase, during which alerts were issued if participants remained non-attentive for approximately 8 consecutive seconds. A paired t-test ($t = 5.73$, $p = 0.007$) indicated a statistically significant improvement in concentration during the feedback phase.

Index Terms—brain-computer interface (BCI), electroencephalography (EEG), machine learning (ML), support vector machine (SVM)

I. INTRODUCTION

CONCENTRATION monitoring has become essential to ensure learning effectiveness in online classes, whose adoption has been steadily increasing across different educational curricula [1]. Prior research shows that learners are more prone to mind-wandering when they are watching lecture videos (being regarded as online learning scenario) than during live lectures (traditional offline classes) [2]. Thus, to track the engagement of students in educational and learning settings, conventional methods of developing questionnaires [3] or camera-based monitoring [4], [5] are used. Although questionnaires are useful for objective evaluation of students, they only serve as a manual tool that requires human intervention and input. Conversely, webcam-based monitoring systems are limited to analyzing external behavioral cues such as facial expressions, gaze, or posture, and therefore lack the ability to provide direct neurophysiological insights into

learners’ cognitive attention levels [6], alongside inducing privacy issues [7]. Additionally, vision-based models fail to preserve robustness in low-light conditions. For this reason, Brain-Computer Interface (BCI) has emerged as a powerful tool to perform cognitive load evaluation of students while watching lecture videos.

BCI is a form of neurotechnology that is leveraged to establish a direct connection between humans and machines. Specifically, electroencephalography (EEG) signals are increasingly being utilized for various use cases, including bionic intelligence [8], vehicle control [9]–[11], and other assistive technologies [12]–[14]. BCI has gained considerable recognition in the classification of attentive and non-attentive states [15] including distraction [16] and drowsiness [17]. Despite the fact that this article is particularly oriented to enhance concentration levels, terms like focus, attention, concentration, and engagement, which are different constructs overlapping each other, can be used interchangeably as the goal is to improve online learning for students using BCI. It has been seen from studies that the prefrontal cortex plays a crucial role in evaluating sustained attention [18]–[20]. In the frontal region, the features contributing to concentration level detection are predominantly the changes in delta, theta, alpha, and beta band power. [18], [19], [21].

Current state-of-the-art works use EEG devices for laboratory experimentation that are not fully consumer-grade which makes them not suitable for real-time implementation. Some of them are Emotiv Insight, Emotiv EPOC+, and OpenBCI Ultracortex. These devices lack dry electrodes, requires accurate placement across multiple scalp regions, not cost-effective and present setup challenges for consumers [22], [23]. Among consumer-grade devices, cost-effective options such as Muse, NeuroSky MindWave, and FocusCalm have been studied. However, existing works provide limited details about their data collection strategies in online learning scenarios [24]–[27], leaving a gap in collecting ground truth (referring to correct labeling of neural data containing actual concentration and actual non-concentration states). Other consumer-grade devices from companies such as Cognionics and Wearable Sensing have been promoted for use in sports scenarios but their high cost and large number of electrodes reduce their suitability for consumer-friendly applications in this field. Vital gaps are seen in real-time implementation of BCI research articulated to track concentration of students in learning environments. Huang et al. [28] have focused on real-time cognitive monitoring to improve concentration time with neuro-feedback mechanism. However, the data collection strategy included mental arithmetic tasks which is not an identical simulation

of learning environment and the data validation has been done using post regulation assessments such as Sustained Attention to Response Task (SART) [29], which cannot validate the participants' engagement during the mental arithmetic tasks. Furthermore, the working algorithm of the single-channel EEG headband, along with the feature extraction and model training process, has not been discussed, as their work focuses more on evaluating the effects of neurofeedback rather than on developing the classification methodology. Conrad and Newman have developed a strategy to use EEG signals for evaluating mind-wandering in online classes [30]. However, the use of only pre- and post-assessment questionnaires is insufficient to validate learners' attention levels during the video. The work done by Rehman et al. [31] relied on publicly available datasets which poses the same limitations as the earlier research gaps. The studies summarized in Table I were selected to represent existing approaches for monitoring learner attention in online learning environments. Inclusion criteria were works that addressed learner engagement or attention in online or remote learning settings, and use of other related modalities (e.g., webcam-based, neurofeedback) whose limitations are being addressed in our proposed approach. Exclusion criteria included works focusing purely on offline classroom learning, cognitive tasks unrelated to learning (e.g., driving simulators), or studies that did not explicitly address attention/engagement measurement.

TABLE I
SUMMARY OF PRIOR STUDIES

Work	Focus	Limitations
Camelia [3]	Questionnaire to validate learner engagement	Requires manual interventions
Patil [4] and Hossen [5]	Computer Vision (webcam) to understand learner engagement	Lack of insights in cognitive processing
Huang [28]	Validating the effects of neurofeedback in increasing attention span	Lack of proper documentation on classification algorithm
Conrad [30]	Evaluating mind-wandering of students in online classes using EEG	Lack of proper data validation techniques
Rehman [31]	Attention classification using their Deep Q-Learning model	Computationally intensive and less feasible for real-time implementation

In this study, a eeg based attention classification framework has been proposed to address the research gaps, with a focus on real-time implementation in online learning scenarios. A novel data acquisition and validation design through intra-video questionnaire assessment has been done to label the blocks as ground truths. The experimentation has been done on classifying two cognitive states of students, namely attention and non-attention. Twenty participants were recruited to participate in data collection experiments containing two sessions, designated for the two classes of data and the device used is a FocusCalm headband. After that, several preprocessing techniques have been employed to get clean data, followed by feature extraction, feature selection and classification. Following this, leave-one-subject-out validation

has been done in order to evaluate the classifier model when faced with unseen data. Finally a simple app GUI has been developed to have real-time insights of concentration levels along with a feedback mechanism to alert the learner during non-attention states. Thus, this article has contributions in the following areas:

- A data collection paradigm has been introduced that uses authentic lecture videos from educational technology platforms as EEG stimuli, offering a closer approximation to real-world online learning environments than traditional controlled tasks.
- A novel intra-video questionnaire assessment has been proposed for data validation, which, unlike traditional post-task questionnaires or external measures (e.g., SART), collects learner responses during the lecture itself. This approach minimizes recall bias, provides time-specific ground-truth labels, and enhances the reliability of the EEG dataset.
- A real-time system has been developed with feedback alerts to ensure the attention spans of learners improve over time. A preliminary evidence of its effectiveness in enhancing concentration is validated via a pilot study.

II. DATA COLLECTION

In this section, a detailed explanation of the inclusion criteria of participants, device used for data collection, experimental design and setup is given.

A. Participant Selection

A total of 20 students with a mean age of 22.8 ± 3.8 years have been recruited for the data collection experiment. A detailed explanation of the experimental setup, collection paradigm and the study has been given to the participants before taking their informed consents. Participants retained the right to leave the data collection process at their discretion at any moment. This data collection protocol has been approved by the Institutional Research Ethics Board (IREB), United International University (UIU). Among the participants, 15 are graduate students of Advanced Intelligent Multidisciplinary System Lab (AIMS Lab) under Institute of Research, Innovation, Incubation & Commercialization (IRIIC), UIU and rest are the students of UIU. They have been selected to pass the condition of having cognitive abilities necessary to comprehend standard high school or equivalent curriculum-based educational material. This has been ensured due to the video stimuli being exposed to the participants at the time of data collection containing online lectures on different topics prepared by national educational technology platforms.

B. Data Acquisition Device

FocusCalm headband [32] has been used as the data acquisition device in this work for its consumer-grade accessibility, dry electrode system, frontal EEG coverage, low setup complexity and a balanced trade-off between signal quality and user comfort. It is a neuro-feedback EEG device designed for meditation purposes. There are three dry electrodes placed

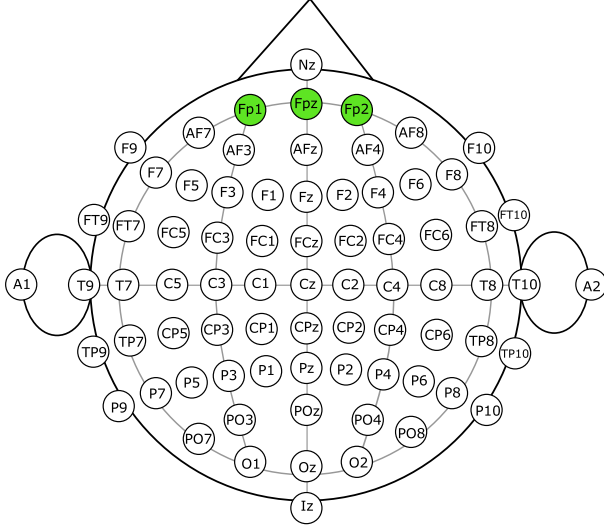


Fig. 1. Positions of Fpz, Fp1 and Fp2 electrodes used by FocusCalm headband according to the international 10-10 electrode placement system.

close to each other and aligns with the Fp1, Fp2 and Fpz positions of the international 10-10 electrode placement system as shown in Fig. 1. Fpz is used as the primary electrode, while Fp1 and Fp2 serve as the reference and ground electrodes [33]. The device wirelessly sends single channel data at 250 Hz along with eight distinct values of which six indicate the delta, theta, alpha, low beta, high beta and gamma frequency band values and the other two shows attention and meditation scores given by their developed model. The developers of FocusCalm at BrainCoTech has made a software development kit (SDK) named Crimson SDK which is accessible for taking raw eeg data along with the eight other values in real-time.

C. Data Collection Experiment

The data collection experiment has been designed using the Psychopy software [34]. The design included a starting instructional video for both classes (attentive and non-attentive) that gives a brief view of the experiment done.

The participants are asked to watch a 10 minutes long video lecture that has been splitted into blocks of 30 seconds mean duration. Subsequently, a question on that exact block will be showed on the screen with multiple choices which the participants have to answer. The duration given for answering the question has been set to 15 seconds as participants take around 4 to 5 seconds for reading a sentence [35]. This gives the participants 10 seconds to answer which is ample considered that humans take around 2 seconds to recognize answers [36]. The questions have been set to ensure that the participant has followed the lecturer's quotes and drawings on the board. The questions require no external knowledge to be answered in order to ensure objective evaluation of a participant's engagement. After the instructional video, a short sample video is played followed by a question answer block to make the participant get accustomed to the experiment. A conditional screen is played with a fixation cross where the participant has to press a key to start the video lecture. In this way, each participant had to watch 20 video blocks

of a lecture followed by questions inserted between them. The experimental setup captures timestamps which mark the start and end of each video block together with participants' responses to the questions. These records are subsequently used for data validation.

For the non-attentive data collection session, similar video sequences are presented but rendered inaudible and blurred to prevent participants from perceiving the content. The participants were instructed to stare at the screen for 5 minutes followed by 5 minutes with eyes closed. In the eyes-open condition, participants viewed the hazy, non-informative video intended to provide minimal external stimulation and thereby facilitate mind-wandering, a common occurrence in real-world scenarios where students face difficulties in maintaining attention during online lectures. The eyes-closed condition has been designed to simulate drowsiness or dozing off during online lectures. A brief overview has been illustrated in Fig. 2a.

D. Data Validation

After successful data acquisition, the eeg data are stored with proper timestamps through some modifications of the Crimson SDK and the responses to the questions are stored with synchronized timestamps. The correct response to a question from the participants validates the EEG data corresponding to the video block that the question succeeds. All the validated blocks are stored as ground truths for attentive data. For non-attentive data, the questionnaire assessment is not done and thus require no further validation. The procedure has been shown in Fig. 2b.

III. METHODS

The validated data is processed through several steps namely data pre-processing, feature extraction and feature selection before being used as training data for classification.

A. Data Preprocessing and Preparation

Data is pre-processed through steps that include segmentation, filtering, noise removal and smoothing.

1) *Segmentation*: EEG data of each participant of a total length of T samples is partitioned to get data segments of optimal length $L = 1750$ samples (details in section III.D). Although the average sampling frequency of 250 Hz is retained, samples have been considered instead of time intervals due to minute temporal delays in packet transmission that complicate timestamp-based calculations. Through validation, K number of blocks are selected from the initially acquired n blocks for each participant. This number corresponds to the average number of questions (around 20) set for a video lecture per session. Sliding window has been used during segmentation to reduce the edge effects and improve statistical reliability [37]. The sliding window is also referred in this article through overlap ratio $r = 0.7$ (details in section III.D). The total number of segments found for each selected block is:

$$n_k = \left\lfloor \frac{T_k - L}{L(1 - r)} \right\rfloor + 1$$

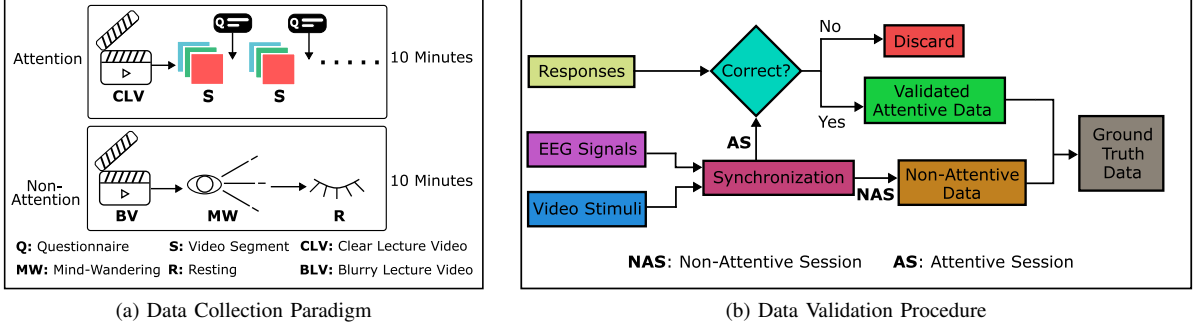


Fig. 2. Overview of the data collection paradigm and validation procedure.

Thus, the total number of segments found is:

$$n = \sum_{k=1}^K n_k = \sum_{k=1}^K \left(\left\lfloor \frac{T_k - L}{L(1-r)} \right\rfloor + 1 \right)$$

And the total number of samples are $x = n \times L$. During segmentation, two columns have been added for labeling and assigning subject-wise user_ids. These will be used later in classification.

To ensure subject-wise label balance, samples with both labels have been extracted separately for each subject. Let \mathcal{D}_u^0 and \mathcal{D}_u^1 denote the sets of samples with labels 0 and 1 respectively (0 meaning attentive and 1 meaning non-attentive), for a given user u . An equal number of samples are retained by trimming the larger class to match the size of the smaller one. Number of samples to be retained, $n_u = \min(|\mathcal{D}_u^0|, |\mathcal{D}_u^1|)$, and the last n_u samples from each label set are selected, which gives $\mathcal{D}_{u,\text{tail}}^0(n_u)$ and $\mathcal{D}_{u,\text{tail}}^1(n_u)$. The balanced dataset for user u is then

$$\mathcal{B}_u = \mathcal{D}_{u,\text{tail}}^0(n_u) \cup \mathcal{D}_{u,\text{tail}}^1(n_u),$$

and the final dataset is

$$\mathcal{B} = \bigcup_{u \in \mathcal{U}} \mathcal{B}_u$$

Given that the dataset retains a substantial number of segments, class imbalance is addressed by trimming the larger class rather than oversampling the smaller one.

2) *Filtering*: The EEG signals have been filtered using a bidirectional Butterworth bandpass with a cutoff frequency of 0.5–64 Hz as a standard range in this research field with an optimal order of 3 found through graphical comparisons. The problem arises due to edge effects caused by filter initialization and group delay as seen in Fig. 3a. To overcome this, 250 samples have been trimmed from both ends of each segment to get clean signal with almost no phase distortion after the filtering is done. The procedure can be visualized from Fig. 3b. This method adds a constraint to the selection of segment length for experimentation which is $L > 500$ samples. This means that the new segments found after trimming will have a length of $(L - 500)$ samples which gives another constraint of setting the ratio r . The constraint can be understood as $r \times L > 500$. The logical explanation can be understood from the overall segmentation and trimming procedure as given in Fig. 3c where the sequential overlapping and trimming of the segments are shown along with the obtained segments. Then

the signal is passed through a notch filter of 50 Hz to avoid power line interference.

3) *Artifact Removal*: Non-invasive EEG signals are often contaminated by artifacts, including eye blinks. Two steps have been followed in this research for noise removal. First, the filtered segments are checked for high-amplitude values greater than a threshold of $150 \mu\text{V}$ as meaningful EEG data lie below this value [38]. If any segment contains at least one high amplitude value, then that segment is dropped from the dataset. Correlation and interpolation are commonly used for high-amplitude portions [39], [40], but the segment rejection approach has been used here to exclude artificial continuations, especially given the abundance of collected data. Following this, eye blinks are removed through Ensemble Empirical Mode Decomposition (EEMD) [41]. Peak indices are extracted from the filtered EEG signal using the `find_peaks` function from the SciPy library [42]. Then three conditions have been imposed to taking the region around the peak. If a peak index falls within the starting 40 or ending 80 values of the segment, then the starting 120 or ending 120 values are taken for EEMD. However, if the peak index falls within the rest of the region then the 40 values before and 80 values after the peak index are taken. These indices are taken from rigorous experimentation to get optimal artifact removal. The signal found after doing EEMD is passed through an uniform filter to smooth residual high-frequency noise.

B. Feature Extraction

Following pre-processing, feature extraction is applied to the segments. A comprehensive set of 458 features have been extracted from the EEG signals to capture time-domain, frequency-domain, wavelet-domain, and statistical characteristics. Time-domain features included commonly used descriptors such as Hjorth parameters (e.g., complexity, activity), median (md), normalized second difference (n2d) etc. Frequency-domain features encompassed spectral moments (e.g., centroid, spread), entropy-based measures, and spectral shape descriptors (e.g., crest, flatness, roll-off). Additionally, wavelet packet transform (WPT) has been used to extract sub-band energy and entropy features which captures localized time-frequency dynamics. These features have been selected based on their proven effectiveness in attention evaluation through EEG and biosignal analysis. Eight additional features obtained from the Crimson SDK have been appended to

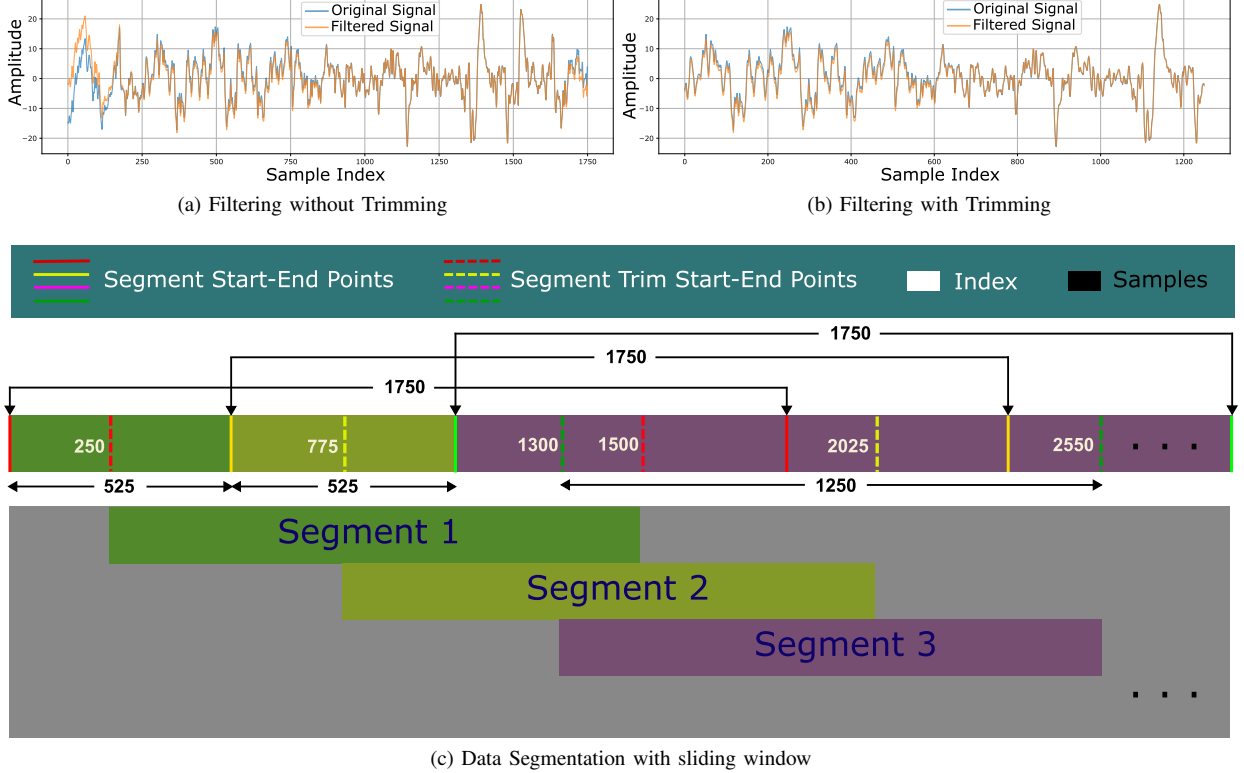


Fig. 3. Subfigures (a) and (b) illustrate the effect of trimming on filtered EEG signals, showing signals without trimming in (a) and with trimming in (b). Subfigure (c) presents the data segmentation pipeline using overlapping windows, highlighting how trimming affects the resulting segments.

the initial 458 features, resulting in a total of 466 features. These include six frequency band powers of the raw EEG signal, along with attention and meditation scores for each segment. As these features are readily available through the open-source Crimson SDK and have been commercially utilized, they are included in the feature set to explore their potential contribution to the classification task. After feature extraction, all computed feature matrices are examined for invalid values. Such invalid values can arise from divisions by zero or logarithmic transformations of zero-valued data, particularly in spectral features. Any features containing NaN (Not a Number) or infinite (Inf) values are identified and replaced with zero. Zero has been used as it preserves dimensionality, enables batch processing, and acts as a neutral, non-informative value without introducing imputation bias. This step ensures numerical stability and prevents errors in subsequent processing and model training.

C. Feature Selection

The next step after feature extraction is selection of most relevant features for training the data. This is necessary to ensure that the final model is trained on the best set of features that contributes to the classification performance. The selection has been done in two steps: Pearson correlation filtering (PCF), followed by Recursive Feature Elimination (RFE) using Support Vector Machine (SVM).

1) *Pearson Correlation Filtering*: PCF has been used to reduce high dimensionality and optimize computational effi-

ciency which works through selecting one from each highly correlated pair when the coefficient of correlation exceeds a threshold p . The value of $p = 0.8$ (details in section III.D) has been used to remove the highly correlated features, leaving 108 in the set for further analysis. The Pearson correlation coefficient is defined as:

$$r_{xy} = \frac{\sum_{i=1}^n (x_i - \bar{x})(y_i - \bar{y})}{\sqrt{\sum_{i=1}^n (x_i - \bar{x})^2} \sqrt{\sum_{i=1}^n (y_i - \bar{y})^2}}$$

where x and y are the features, \bar{x}, \bar{y} are their means and n represents the number of paired observations.

2) *Recursive Feature Elimination with SVM*: Subsequently, RFE with SVM has been exploited to find the meaningful set of features required for optimal model training. It is a supervised feature selection method that removes the least important features recursively based on the weights assigned by a linear SVM model. At each iteration, the model is trained on the current feature set, and features with the smallest absolute weights (least contribution to the decision function) are eliminated. This process continues until the desired number of features $d = 50$ (details in section III.D) is retained.

First, RFE has been applied for each subject (identified by user_id) using the linear SVM. The regularization parameter C_1 for this SVM has been iterated through a range (0.01 to 100), to account for varied model complexity and feature importance. For each C_1 value, a set of 50 top-ranked features is obtained. These sets are not directly finalized but evaluated through another SVM with radial basis function (RBF) kernel. The classification performance of this secondary model serves

as the basis for selecting the optimal feature set. This subject-focused process has been designed so that the selected features are not only ranked high based on linear separability but also demonstrate better generalization of the model. Finally, a set of 9 common features is obtained through finding the most frequently selected features across all subjects. Out of these features, the relative powers of alpha and delta band, ratio of low beta to summation of alpha and theta band, average power of low beta band, and median of high beta band show strong correlations with those reported in the literature as contributing to sustained attention [18]–[21]. These consensus-based features have been used for final model training. The selected features for final training along with their meanings are given in Table II.

TABLE II
SELECTED FEATURES FOR TRAINING

Feature	Meaning
RP_A	Relative power of alpha band
RP_D	Relative power of delta band
attention	Attention Score from Crimson SDK
avg_pow_B1	Average power of low beta band
en_b_at	Ratio of low beta to summation of alpha and theta band
hc_D	Hjorth complexity of delta band
md_B2	Median of high beta band
meditation	Meditation Score from Crimson SDK
n2d_G	Normalized second difference of gamma band

D. Hyperparameter Tuning

All parameters defined from pre-processing to feature selection have been systematically varied to evaluate their impact on classification performance through rigorous assessments. For segment length L , values ranging from 5 to 8 paired with overlap ratios ranging from 0.3 to 0.7 have been used for analysis. The pair of $(L, r) = (1750, 0.7)$ has been found to be optimal through comparisons of model performance across all tested values. Similar approach has been followed for Pearson correlation coefficient threshold P (0.6 to 0.95 in increments of 0.05) and optimal number of features d (30 to 80 in increments of 10). The best trade-off between model performance and generalization has been found for $P = 0.8$ $d = 50$. For RFE, the linear SVM has been trained on $C_1 \in \{0.01, 0.1, 1, 10, 100\}$ and the secondary SVM for identification of optimal feature set has been trained on a nested grid search of two parameters $C_2 \in \{0.01, 0.1, 1, 10, 100\}$ and $\gamma \in \{0.001, 0.01, 0.1, 0.5, 1, 10\}$. The combination yielding the highest performance determines the best feature set corresponding to the optimal C_1 . Final classification is also tuned using a separate grid search on the same range of C_2 and γ which is applied on the common features obtained across all users. The optimal pair of $(C_2, \gamma) = (0.01, 0.5)$ has been found to yield the best classification performance.

E. Classification

SVMs have been widely adopted for EEG classification tasks due to their robustness in high-dimensional spaces, effectiveness with small sample sizes, and ability to articulate non-linear decision boundaries through kernel functions. Thus,

an SVM with RBF kernel has been selected for capturing non-linear relationships in the feature space. The SVM finds a hyperplane that maximizes the margin between classes while allowing some misclassifications which is controlled by the regularization parameter C_2 . The kernel coefficient γ determines the influence of individual training samples on the decision boundary, shaping how tightly the model fits local patterns in the feature space.

The training pipeline as explained in Algorithm 1 includes fitting the model on a nested grid search of C_2 and γ . The evaluation is performed through leave-one-subject-out (LOSO) cross-validation. LOSO is an appropriate choice to effectively assess the model's generalizability on unseen subjects which closely reflects real-world application scenarios.

Algorithm 1: Model Training And Validation Using LOSO

```

Input: Dataset  $\mathcal{D}$  with subject labels user_id,  

        hyperparameter grids  $\mathcal{C}_2, \Gamma$   

Output: Optimal hyperparameters per subject and  

        performance metrics  

1 Obtain set of unique subjects  $U$  from  $\mathcal{D}$  ;  

2 foreach  $subject u_{test} \in U$  do  

3    $\mathcal{D}_{test} \leftarrow$  data from  $u_{test}$  ;  

4    $\mathcal{D}_{train} \leftarrow \mathcal{D} \setminus \mathcal{D}_{test}$  ;  

   // Nested grid search on training  

   data  

5   Initialize best_score  $\leftarrow 0$  ;  

6   foreach  $C_2 \in \mathcal{C}_2$  do  

7     foreach  $\gamma \in \Gamma$  do  

8       Train SVM with RBF kernel using  $(C_2, \gamma)$   

       on  $\mathcal{D}_{train}$  ;  

9       Evaluate on  $\mathcal{D}_{test}$  to get score ;  

10      if  $score > best\_score$  then  

11         $best\_score \leftarrow score$  ;  

12        Save  $(C_2, \gamma)$  as optimal for  $u_{test}$  ;  

13   Store best score and best  $(C_2, \gamma)$  for  $u_{test}$  ;  

14 Compute average performance across all subjects ;

```

After a rigorous grid search, the pairs of C_2 and γ yielding the best classification performance for the subjects are recorded. From these pairs, the most frequent one is selected for fitting the final model which is then used for real-time evaluation.

F. Evaluation Metrics

The performance of the classifier has been evaluated using standard metrics including accuracy, precision, recall, and F1-score. As the dataset has been balanced per class during segmentation, these four metrics are sufficient for evaluating the model performance.

IV. EXPERIMENTAL RESULTS

This section provides the performance evaluation of the trained model and the ablation studies that have led to its optimized version.

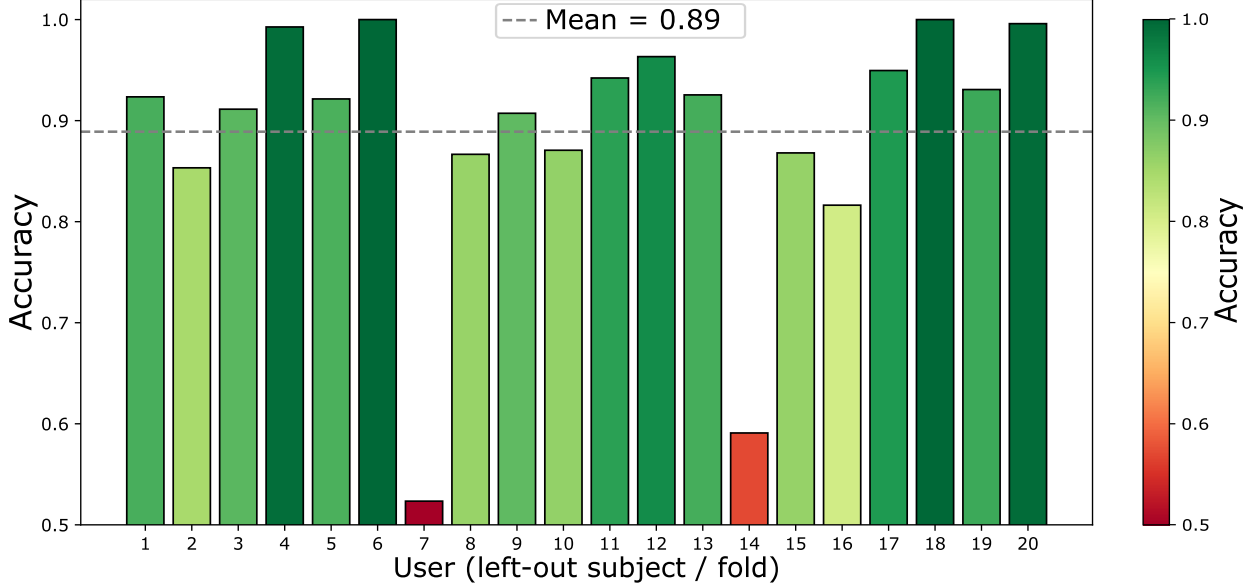


Fig. 4. Accuracy of the model evaluated using Leave-One-Subject-Out (LOSO) cross-validation, where each iteration treats one subject as the test fold and the remaining subjects as the training set.

A. Cross-Validation Results

The model performance has been analyzed using the LOSO cross-validation procedure (discussed in section III.E). The optimized model performance on each fold (fold implying the data of each subject as test data while taking all the others as train data) has been shown in Fig. 4. The optimized model achieves the average test accuracy of 88.77%. Additionally, it attains a precision of 90.49%, recall of 88.77%, and F1 score of 89.03% which indicates strong predictive capability with a good balance between correctly identifying positive cases and minimizing false positives.

B. Model Ablation Studies

Initially, 458 features excluding the 8 features provided by the Crimson SDK, are used to train the SVM which gave an accuracy of 76.44%. Subsequently, the 8 SDK features are incorporated, and the model is retrained, achieving the current best performance. Among these additional features, the attention and meditation scores are included in the final feature set. To assess whether the model's performance is overly reliant on these two scores, it has been compared against the baseline performance obtained using only the Crimson SDK's scores as the feature set. Crimson SDK has been selected as the baseline as it gives the scores which are associated with cognitive load. To have the accuracy from those scores as predictions to the EEG signals, two methods have been employed. The first method includes training the model on the two features and evaluating the metrics, which gave an accuracy of 84.13%. The second method involves the ratio of attention to meditation score r_{am} as the condition to classify the data. For all the n segments found, the predictions have been taken to be attentive if $r_{am} > 1$ and non-attentive otherwise. The accuracy is found to be 82.27%. This shows that the proposed methodology outperforms the current interface of

the FocusCalm headband modified for attention classification in online learning environments (details discussed in section V). A brief summary has been given in Table III for a clear overview.

TABLE III
MODEL ABLATION PERFORMANCE

Method	Performance
458 features excluding attention and meditation scores	76.44%
Ratio of attention and Meditation scores	82.27%
Attention and meditation scores as final features	84.13%
466 features including attention and meditation scores	88.77%

V. DISCUSSION

The overall research methodology differs from baseline methods (given the limited prior research addressing this objective within this specific environment). Therefore, the discussion focuses on the unique aspects of the approach, the rationale for their selection, their implementation, and the specific methods they outperform. Also, the limitations of the current research along with logical representations have been mentioned.

The proposed EEG-based attention classification achieves 6.5% better accuracy than the Crimson SDK, which suggests that the combination of wavelet packet decomposition along with entropy features are effective in capturing attention state dynamics. Although baseline methods achieve satisfactory results, the data collection strategies of other baseline studies such as Rehman et al. and Huang et al. are based on instructions and there remained a room for data validation strategies which have been implemented in this research. The steps followed in this research ensure correct predictions which pertains to ground truths and this is crucial for real-time implementation.

Initially, device selection was emphasized, as most previous research has relied on non-consumer-grade devices. For this study, the FocusCalm headband has been chosen for its portability, wearability, and ease of hands-on use, despite the potential for experiments with the Muse headband, which offers greater spatial coverage in real-time applications. Given our objective of developing a state-of-the-art real-time binary classification system, the FocusCalm device has proven sufficient for our purposes. The data collection protocol was designed to reflect the environmental setting of classrooms, with video stimuli consisting of lecture content prepared for students. The data validation process was established under the principle that only ground-truth labels are required. Instances can occur where a participant experiences cognitive load yet fails to answer a question. However, this does not affect labeling, as the protocol ensures that all selected data correspond to verified ground truths.

The methods used in this research were selected through extensive trials of different approach combinations. For instance, both causal forward filtering and zero-phase second-order section (SOS) filtering were tested. While the latter removed phase distortion more effectively, it performed poorly at the start and end of segments during segment-wise processing, as it requires future data to operate. To address this, those edge portions were removed, ensuring both the absence of distortion and the independence from future data. Furthermore, to prevent data loss, the segmentation process used an overlapping ratio that retained common portions between consecutive segments. For classification, SVM was initially selected due to its proven effectiveness in EEG signal analysis. Conceptually, SVM can be viewed as a mechanism that iteratively identifies the most discriminative features in a high-dimensional space, analogous to how traditional EEG analyses iteratively isolate regions or frequency bands of interest to distinguish cognitive states. An initial assessment using various machine learning models was conducted, and the SVM achieved the highest performance, which is consistent with observations reported in the literature.

After validating the data using LOSO, the optimal (C_2, γ) values were determined in two ways. The first method identified the most common (C_2, γ) pair that achieved the best metrics across all subjects. The second method selected the (C_2, γ) pair that yielded the highest metrics, regardless of its frequency among subjects. The mode pair, $(C_2, \gamma) = (0.01, 0.5)$, produced an average accuracy of 88.77%, whereas $(C_2, \gamma) = (0.01, 0.1)$ achieved a slightly higher average accuracy of 89.63%. Despite the higher accuracy, the former pair was adopted for real-time testing due to its more frequent favorable performance, which makes the model generalized and objective. Another key finding from the LOSO validation results was the model's relatively poor performance on two subjects when taken as test set, although it has achieved satisfactory classification results for the other subjects as shown in Fig. 4. This indicates that the model can be made more robust by incorporating additional data.

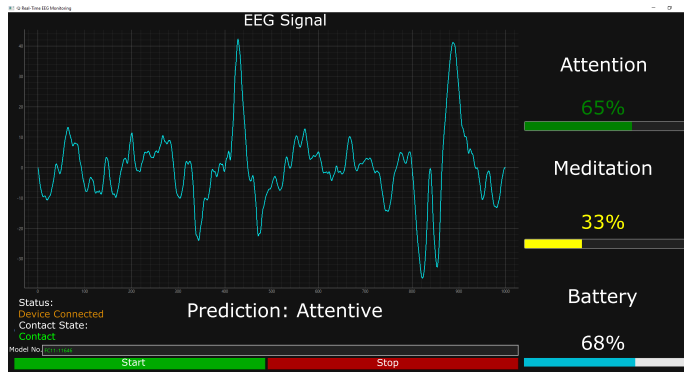
VI. REALTIME SETUP

A. Data-handling Procedure

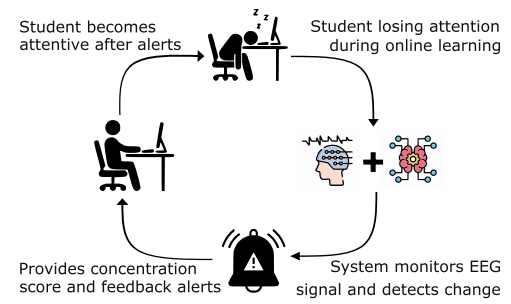
The real-time implementation has been done through building a software interface in python. The raw EEG data stream from the headband device is handled using a circular buffer mechanism to ensure continuous real-time processing without data loss or overlap. A fixed-size buffer of capacity $B_C = 10000$ is allocated to store incoming EEG samples, along with parallel buffers to record the corresponding attention and meditation metrics. This capacity is chosen to accommodate multiple segments while maintaining an effective trade-off between memory utilization and processing efficiency. Incoming EEG data packets are appended to the buffer. When the insertion point approaches the end of the buffer, the packet is split and wrapped around to the buffer's beginning, ensuring efficient circular memory usage. This approach prevents overwriting unread data and maintains temporal continuity. A read pointer tracks the start position of data segments ready for analysis. Data availability is monitored by a counter that tracks the total unread samples in the buffer. Once the accumulated unread data reaches or exceeds a predefined window size of 1750 samples (length of segment), the application extracts fixed-length EEG segments for processing. After each window prediction, the read pointer advances a step size of 525 samples (to maintain the same overlap ratio of 0.7 for producing segments of training data), meaning that the window size is filled and processed every 2.1 seconds approximately. Segments are extracted with potential wrap-around handling which implies that, if the segment spans the end of the buffer, it is reconstructed by concatenating the tail portion with the head of the buffer to maintain continuity. In the processing function, the noise removal, feature extraction and classification using the trained model is done. Following this, the read pointer advances by a defined step size, and the unread data count decreases accordingly, supporting overlapping window analysis and ensuring no data gaps.

B. Graphical User Interface Development

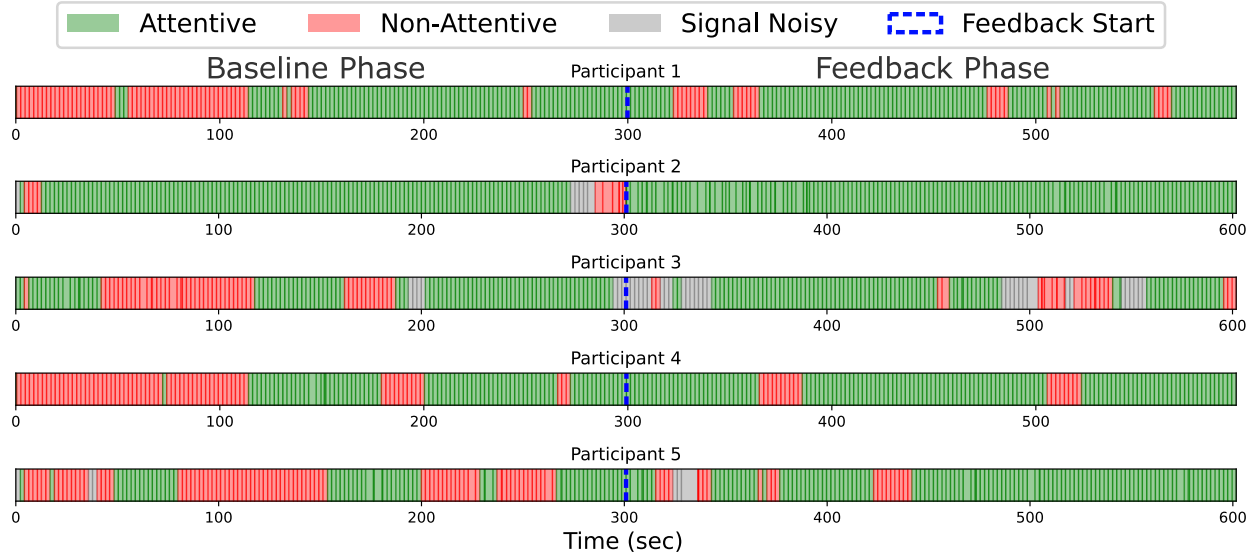
The software's graphical user interface (GUI) was developed using PyQt6. It displays the raw EEG signal in real time, along with the attention and meditation scores from the Crimson SDK, the proposed algorithm's prediction, the headband's battery level, and its contact state. An input box is provided to enter the model of the specific headband, along with a Connect button to establish the connection. After connecting the headband and starting the algorithm, if non-attention is detected for five segments consecutively, an alert sound is played and an on-screen warning reminds the subject to concentrate. If contact with the headband is lost, a similar warning prompts the subject to adjust it. For segments with significant artifacts, a message in the GUI indicates that the signal is noisy. When the Stop button is pressed at the end of a session, a summary is displayed showing detailed statistics of attention and non-attention over time. This ensures interactive communication with the subject while minimizing interventions. Therefore better cognitive engagement with the video is promoted and attention span is improved. The developed graphical user



(a) Graphical user interface (GUI) for real-time EEG data visualization and classification.



(b) Overview of the online learning pipeline, showing EEG signal acquisition, real-time classification, and neurofeedback to regain attention.



(c) Graphical visualization of cognitive states in two phases of conducted pilot study.

Fig. 5. Subfigures (a) and (b) represents the graphical user interface and the real-time working pipeline. Subfigure (c) denotes the changes between attentive and non-attentive states during the real-time system test on five participants.

interface has been illustrated in Fig. 5a. Additionally, the working pipeline of the real-time feedback incorporated with online learning environment can be visualized from Fig. 5b. It can be seen that the student is alerted when attention is lost during online learning environments. The overall methodology helps in this feedback and the student regains concentration again.

C. Pilot Evaluation

To preliminarily assess the effectiveness of the implemented feedback mechanism, a pilot study was conducted involving five participants. Each participant underwent a 10-minute session where a video stimuli of an educational lecture was given. The session consisted of two consecutive phases: a 5-minute baseline phase without feedback and a 5-minute feedback phase. During the baseline phase, the system continuously monitored cognitive states of the participant without any visual or audio alerts on non-attentive state detection. For the feedback phase, the same monitoring was done and the system issued visual and audio alerts whenever a participant

remained non-attentive as per the model for approximately 8.4 consecutive seconds (4 overlapped segments).

A paired t-test was conducted on the mean durations of non-attentive states in the two phases. At first, the durations of continuous non-attentive states have been calculated and segments having less than 8 seconds duration has been discarded as the effect of feedback mechanism is being evaluated. The paired t-test yielded a t-statistic of 5.73, and a p-value of 0.007. Moreover, the mean duration of non-attention periods for the participants has been found to be 37.50 seconds in the baseline phases and 14.97 seconds in the feedback phases. Both analyses indicated a significant improvement in concentration during the feedback phase, suggesting that the real-time alerts effectively supported participants in regaining and sustaining attention. Fig. 5c gives a graphical overview for better visualization, portraying the timeline of sustained non-attention in the baseline phase and the feedback phase.

VII. CONCLUSION

As traditional methods like questionnaire and observations require manual interventions, they are not suitable for online

learning. For this reason, an automated real-time attention classification with neurofeedback mechanism has been developed in this article. The methodology includes data collection through the FocusCalm headband, data preprocessing including segmentation with a sliding window, filtering, and high amplitude artifact removal, feature extraction and selection, and classification. The proposed algorithm achieved an average accuracy of 88.77% on leave-one-subject-out validation, which proves the robustness of the model when faced with unseen test data.

Future work will focus on expanding the dataset to include a more diverse participant pool. Better and more robust methods will be developed to ensure better performance of the model without requiring the attention and meditation scores of the Crimson SDK. The application will be analyzed through implementation in multiple use cases, followed by systematic result collection. The use of multi-channel, consumer grade and ready-to-use EEG devices will be adopted for better spatial coverage to capture and classify visual, auditory, and task distractions alongside attention and drowsy states in learning environments. Another possible implication is integrating this research with multi-modal inputs such as facial expressions and behavioral logs, to evaluate the key dimensions of a class: learner engagement and content quality. This research thus paves the way for practical and scalable real-time BCI applications in education and beyond.

ACKNOWLEDGMENTS

We gratefully acknowledge the Advanced Intelligent Multidisciplinary Systems Lab, under the Institute of Research, Innovation, Incubation & Commercialization at United International University, for their support and resources, Institute of Advanced Research for funding this project (Code No. UIU-IAR-02-2024-SE-39) and Onnorokom EdTech Limited for testing our project in their learning environment.

REFERENCES

- [1] P. Qiao, X. Zhu, Y. Guo, Y. Sun, and C. Qin, "The development and adoption of online learning in pre- and post-covid-19: Combination of technological system evolution theory and unified theory of acceptance and use of technology," *Journal of Risk and Financial Management*, vol. 14, no. 4, p. 162, Apr. 2021. [Online]. Available: <http://dx.doi.org/10.3390/jrfm14040162>
- [2] J. D. Wammes and D. Smilek, "Examining the influence of lecture format on degree of mind wandering," *Journal of Applied Research in Memory and Cognition*, vol. 6, no. 2, p. 174–184, Jun. 2017. [Online]. Available: <http://dx.doi.org/10.1037/h0101808>
- [3] F. Camelia and T. L. J. Ferris, "Validation studies of a questionnaire developed to measure students' engagement with systems thinking," *IEEE Transactions on Systems, Man, and Cybernetics: Systems*, vol. 48, no. 4, p. 574–585, Apr. 2018. [Online]. Available: <http://dx.doi.org/10.1109/TSMC.2016.2607224>
- [4] S. Patil, A. Jani, D. Jondhale, D. Pathak, and A. S. Savyanavar, "Student's attention and alertness monitoring system using AI," in *2024 MIT Art, Design and Technology School of Computing International Conference (MITADTSocCon)*, IEEE, Apr. 2024, p. 1–6. [Online]. Available: <http://dx.doi.org/10.1109/MITADTSocCon60330.2024.10575441>
- [5] M. K. Hossen and M. S. Uddin, "Attention monitoring of students during online classes using XGBoost classifier," *Computers and Education: Artificial Intelligence*, vol. 5, p. 100191, 2023. [Online]. Available: <http://dx.doi.org/10.1016/j.caei.2023.100191>
- [6] Q. Liu, X. Jiang, and R. Jiang, "Classroom behavior recognition using computer vision: A systematic review," *Sensors*, vol. 25, no. 2, p. 373, Jan. 2025. [Online]. Available: <http://dx.doi.org/10.3390/s25020373>
- [7] S. A. L. Nair and R. K. Megalingam, "Human attention detection system using deep learning and brain–computer interface," *Neural Computing and Applications*, vol. 36, no. 18, p. 10927–10940, Mar. 2024. [Online]. Available: <http://dx.doi.org/10.1007/s00521-024-09628-8>
- [8] R. Wei, C. Hua, J. Chen, D. Mu, and J. Zhao, "Attention-based multiscale tCNN for SSVEP classification and its application to bionic intelligent soft gripper control," *IEEE Transactions on Systems, Man, and Cybernetics: Systems*, p. 1–10, 2025. [Online]. Available: <http://dx.doi.org/10.1109/TSMC.2025.3578533>
- [9] J. Wang, L. Bi, and W. Fei, "Multitask-oriented brain-controlled intelligent vehicle based on human–machine intelligence integration," *IEEE Transactions on Systems, Man, and Cybernetics: Systems*, vol. 53, no. 4, p. 2510–2521, Apr. 2023. [Online]. Available: <http://dx.doi.org/10.1109/TSMC.2022.3212744>
- [10] J. Zhuang, K. Geng, and G. Yin, "Ensemble learning based brain–computer interface system for ground vehicle control," *IEEE Transactions on Systems, Man, and Cybernetics: Systems*, vol. 51, no. 9, p. 5392–5404, Sep. 2021. [Online]. Available: <http://dx.doi.org/10.1109/TSMC.2019.2955478>
- [11] S. Lin, C. Fan, D. Han, Z. Jia, Y. Peng, and S. Kwong, "HATNet: EEG-based hybrid attention transfer learning network for train driver state detection," *IEEE Transactions on Cybernetics*, vol. 55, no. 5, pp. 2437–2450, 2025.
- [12] C.-T. Lin and T.-T. N. Do, "Direct-sense brain–computer interfaces and wearable computers," *IEEE Transactions on Systems, Man, and Cybernetics: Systems*, vol. 51, no. 1, p. 298–312, Jan. 2021. [Online]. Available: <http://dx.doi.org/10.1109/TSMC.2020.3041382>
- [13] W. Dang *et al.*, "Flashlight-Net: A modular convolutional neural network for motor imagery EEG classification," *IEEE Transactions on Systems, Man, and Cybernetics: Systems*, vol. 54, no. 7, p. 4507–4516, Jul. 2024. [Online]. Available: <http://dx.doi.org/10.1109/TSMC.2024.3382828>
- [14] N. Kaongoen, M. Yu, and S. Jo, "Two-factor authentication system using P300 response to a sequence of human photographs," *IEEE Transactions on Systems, Man, and Cybernetics: Systems*, vol. 50, no. 3, p. 1178–1185, Mar. 2020. [Online]. Available: <http://dx.doi.org/10.1109/TSMC.2017.2756673>
- [15] D.-H. Lee, J.-H. Jeong, B.-W. Yu, T.-E. Kam, and S.-W. Lee, "Autonomous system for EEG-based multiple abnormal mental states classification using hybrid deep neural networks under flight environment," *IEEE Transactions on Systems, Man, and Cybernetics: Systems*, vol. 53, no. 10, p. 6426–6437, Oct. 2023. [Online]. Available: <http://dx.doi.org/10.1109/TSMC.2023.3282635>
- [16] Y.-W. Choi, H.-B. Shin, and S.-W. Lee, "Brain-guided self-paced curriculum learning for adaptive human–machine interfaces," *IEEE Transactions on Systems, Man, and Cybernetics: Systems*, vol. 55, no. 7, p. 4693–4704, Jul. 2025. [Online]. Available: <http://dx.doi.org/10.1109/TSMC.2025.3560832>
- [17] T. K. Reddy, V. Arora, V. Gupta, R. Biswas, and L. Behera, "EEG-based drowsiness detection with fuzzy independent phase-locking value representations using Lagrangian-based deep neural networks," *IEEE Transactions on Systems, Man, and Cybernetics: Systems*, vol. 52, no. 1, p. 101–111, Jan. 2022. [Online]. Available: <http://dx.doi.org/10.1109/TSMC.2021.3113823>
- [18] P. K. Sahu and K. Jain, "Sustained attention detection in humans using a prefrontal theta-EEG rhythm," *Cognitive Neurodynamics*, vol. 18, no. 5, p. 2675–2687, May 2024. [Online]. Available: <http://dx.doi.org/10.1007/s11571-024-10113-0>
- [19] P. Kaushik, A. Moye, M. v. Vugt, and P. P. Roy, "Decoding the cognitive states of attention and distraction in a real-life setting using EEG," *Scientific Reports*, vol. 12, no. 1, Nov. 2022. [Online]. Available: <http://dx.doi.org/10.1038/s41598-022-24417-w>
- [20] S. Zhang, Z. Yan, S. Sapkota, S. Zhao, and W. T. Ooi, "Moment-to-moment continuous attention fluctuation monitoring through consumer-grade EEG device," *Sensors*, vol. 21, no. 10, p. 3419, May 2021. [Online]. Available: <http://dx.doi.org/10.3390/s21103419>
- [21] L.-W. Ko, O. Komarov, W. D. Hairston, T.-P. Jung, and C.-T. Lin, "Sustained attention in real classroom settings: An EEG study," *Frontiers in Human Neuroscience*, vol. 11, Jul. 2017. [Online]. Available: <http://dx.doi.org/10.3389/fnhum.2017.00388>
- [22] P. Sawangjai, H. Hompoonsup, P. Leelaarporn, S. Kongwudhikunakorn, and T. Wilairapsitpon, "Consumer grade EEG measuring sensors as research tools: A review," *IEEE Sensors Journal*, vol. 20, no. 8, p. 3996–4024, Apr. 2020. [Online]. Available: <http://dx.doi.org/10.1109/JSEN.2019.2962874>

[23] J. Sabio, N. S. Williams, G. M. McArthur, and N. A. Badcock, "A scoping review on the use of consumer-grade eeg devices for research," *PLOS ONE*, vol. 19, no. 3, p. e0291186, Mar. 2024. [Online]. Available: <http://dx.doi.org/10.1371/journal.pone.0291186>

[24] S. Sudharsan, S. Siddharth, M. Uma, and R. Kaviyaraj, "Learning behavior analysis for personalized E-Learning using EEG signals," in *2024 International Conference on Advances in Computing, Communication and Applied Informatics (ACCAI)*, 2024, pp. 1–9.

[25] G. Ruqeyya and S. M. U. Saeed, "Player engagement classification in mobile games using MUSE headband," in *2022 17th International Conference on Emerging Technologies (ICET)*, 2022, pp. 83–88.

[26] M. Beiramvand, M. Shahbakhti, N. Karttunen, R. Koivula, J. Turunen, and T. Lipping, "Assessment of mental workload using a Transformer network and two prefrontal EEG channels: An unparameterized approach," *IEEE Transactions on Instrumentation and Measurement*, vol. 73, pp. 1–10, 2024.

[27] A. Arsalan, M. Majid, A. R. Butt, and S. M. Anwar, "Classification of perceived mental stress using a commercially available EEG headband," *IEEE Journal of Biomedical and Health Informatics*, vol. 23, no. 6, pp. 2257–2264, 2019.

[28] H. Huang *et al.*, "Real-time attention regulation and cognitive monitoring using a wearable EEG-based BCI," *IEEE Transactions on Biomedical Engineering*, vol. 72, no. 2, p. 716–724, Feb. 2025. [Online]. Available: <http://dx.doi.org/10.1109/TBME.2024.3468351>

[29] I. H. Robertson, T. Manly, J. Andrade, B. T. Baddeley, and J. Yiend, "'Oops!': Performance correlates of everyday attentional failures in traumatic brain injured and normal subjects," *Neuropsychologia*, vol. 35, no. 6, p. 747–758, May 1997. [Online]. Available: [http://dx.doi.org/10.1016/s0028-3932\(97\)00015-8](http://dx.doi.org/10.1016/s0028-3932(97)00015-8)

[30] C. Conrad and A. Newman, "Measuring mind wandering during online lectures assessed with eeg," *Frontiers in Human Neuroscience*, vol. 15, Aug. 2021. [Online]. Available: <http://dx.doi.org/10.3389/fnhum.2021.697532>

[31] A. Ur Rehman, N. Ul Eman, F. Ullah, D. Cacciagrano, L. Mostarda, and N. Raza, "Advanced EEG signal processing and deep Q-Learning for accurate student attention monitoring," *IEEE Access*, vol. 13, p. 47260–47270, 2025. [Online]. Available: <http://dx.doi.org/10.1109/ACCESS.2024.3523225>

[32] K. Flanagan and M. J. Saikia, "Consumer-grade electroencephalogram and functional near-infrared spectroscopy neurofeedback technologies for mental health and wellbeing," *Sensors*, vol. 23, no. 20, p. 8482, Oct. 2023. [Online]. Available: <http://dx.doi.org/10.3390/s23208482>

[33] FocusCalm, "Clinics & consultants," [Online]. Available: <https://focuscalm.com/pages/clinics-consultants>, [Accessed: 18-08-2025].

[34] J. Peirce *et al.*, "PsychoPy2: Experiments in behavior made easy," *Behavior Research Methods*, vol. 51, no. 1, p. 195–203, Feb. 2019. [Online]. Available: <http://dx.doi.org/10.3758/s13428-018-01193-y>

[35] B. Kapteijns and F. Hintz, "Comparing predictors of sentence self-paced reading times: Syntactic complexity versus transitional probability metrics," *PLOS ONE*, vol. 16, no. 7, p. e0254546, Jul. 2021. [Online]. Available: <http://dx.doi.org/10.1371/journal.pone.0254546>

[36] R. Ley and D. Locascio, "Study time, recall time, meaningfulness, and recognition latency in paired-associate learning," *Psychonomic Science*, vol. 28, no. 2, p. 88–90, Feb. 1972. [Online]. Available: <http://dx.doi.org/10.3758/BF03328671>

[37] P. Saideepthi, A. Chowdhury, P. Gaur, and R. B. Pachori, "Sliding window along with EEGNet-based prediction of EEG motor imagery," *IEEE Sensors Journal*, vol. 23, no. 15, p. 17703–17713, Aug. 2023. [Online]. Available: <http://dx.doi.org/10.1109/ISEN.2023.3270281>

[38] Z. He, K. Yang, N. Zhuang, and Y. Zeng, "Processing of affective pictures: A study based on functional connectivity network in the cerebral cortex," *Computational Intelligence and Neuroscience*, vol. 2021, no. 1, Jan. 2021. [Online]. Available: <http://dx.doi.org/10.1155/2021/5582666>

[39] P. S. Ledwidge, C. N. McPherson, L. Faulkenberg, A. Morgan, and G. C. Baylis, "A comparison of approaches for motion artifact removal from wireless mobile EEG during overground running," *Sensors*, vol. 25, no. 15, p. 4810, Aug. 2025. [Online]. Available: <http://dx.doi.org/10.3390/s25154810>

[40] X. Jiang, G.-B. Bian, and Z. Tian, "Removal of artifacts from EEG signals: A review," *Sensors*, vol. 19, no. 5, p. 987, Feb. 2019. [Online]. Available: <http://dx.doi.org/10.3390/s19050987>

[41] Z. WU and N. E. HUANG, "Ensemble empirical mode decomposition: A noise-assisted data analysis method," *Advances in Adaptive Data Analysis*, vol. 01, no. 01, p. 1–41, Jan. 2009. [Online]. Available: <http://dx.doi.org/10.1142/S1793536909000047>

[42] P. Virtanen *et al.*, "SciPy 1.0: Fundamental algorithms for scientific computing in Python," *Nature Methods*, vol. 17, no. 3, p. 261–272, Feb. 2020. [Online]. Available: <http://dx.doi.org/10.1038/s41592-019-0686-2>